

Hydrogenated Graphene: Structures and Surface Work Function

N. Jiao, Chaoyu He, C. X. Zhang and L. Z. Sun*

Laboratory for Quantum Engineering and Micro-Nano Energy Technology, Xiangtan University, Xiangtan 411105, China

lzsun@xtu.edu.cn

Abstract: The structures and surface work functions of graphanes with five fundamental configurations are systematically studied with the density functional theory. We find that, from the point of view of energy, hydrogenated graphene prefer forming the chair graphane than the other ones. The work function and layer thickness of the five structures vary with the hydrogenation, providing important theoretical data for experimental identifying the configurations of graphanes by STM and AFM.

Keywords: Graphene, hydrogenation, graphane, Surface work function.

Introduction

Since the first discovery of grapheme in 2004 [1], graphene based transistors [2-4] have rapidly developed. Graphene is considered as a potential candidate for future nano-electronics owing to their remarkable structural and electronic properties. Graphane, a fully hydrogen functionalized graphene, behaves as a wide gap semiconductor or an insulator [5, 6], which is different from graphene. It means that the electronic band gap of graphene can be tuned by chemical decoration. These results are significant for the application of graphene in nano-electronics. However, the identification of the hydrogenated graphene is still an open question because it is hardly to be observed directly in experiments. In present work, using first-principles calculations, we investigate the structures and the surface work functions of five possible hydrogen decorated graphene [6-8].

Models and Method

The five kinds of graphanes considered in this work are shown in Fig.1. The chair and stirrup structures are shown in Fig.1(a) and Fig.1(b), respectively. There are three kinds of boat structures including boat1, boat2 and boat3 as shown in Fig.1(c), Fig.1(d) and Fig.1(e),

respectively. To obtain the work functions of these graphanes, the Vienna Ab initio Simulation Package (VASP) [9] is adopted to optimize their structures and perform total energy calculations. The kinetic cutoff energy is set to be 500 eV and the Brillouin zone (BZ) is sampled using a 15x15x1 Gamma-centered Monkhorst-Pack grid in our calculations. All systems are fully optimized up to the residual force on every atom is less than 0.01 eV/Å through the conjugate-gradient algorithm.

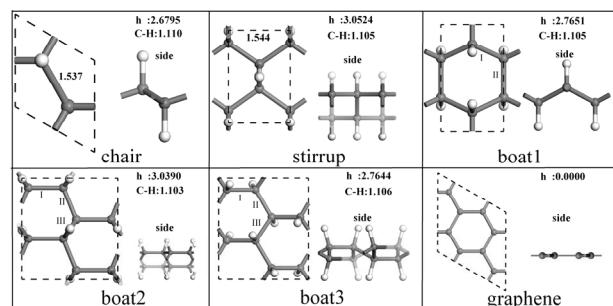


Fig.1: The top and side view of the hydrogenated graphene and the pristine graphene. White is the H atom and gray is the C atom. h is the thickness of the structure. C-H is the bond length between C atom and H atom.

Results and Discussion

The optimized configurations of the five types of hydrogenated graphene and their structural parameters are shown in Fig.1 and Tab.1. We find that the hydrogenated structures, comparing with the sp^2 pristine graphene, become sp^3 hybridization forming a zigzag configuration. All the Gibbs energies of the five configurations are listed in Tab.1. The results of Gibbs energies indicate that the chair structure is the most stable one among the five decorated configurations. After the functionalization, boat2 and boat3

configurations have three types of C-C bond, while boat1 has two types, as shown in Table.1 and Fig.1. The thicknesses (h) of the decorated structures are different, as shown in Tab.1. The chair structure is thinner than the other structures and stirrup is the thickest one. This can be used to identify those two configurations by atomic force microscope (AFM). Comparing with the other boat structures, the h of boat2 is about 0.27Å thicker than boat1 and boat3 structures. This can be distinguished by AFM.

Table.1 Summary of work function and structure properties of the systems studied. Gibbs energy (GE), Work function (WF), Length of the C-C Bond inside the graphene (dc-c).

	Chair	Stirrup	Boat1	Boat2	Boat3	Graphene
GE/ev	-0.103	-0.076	-0.052	-0.039	-0.028	0
WF/ev	3.916	4.407	4.417	4.457	4.543	4.410
dc-c/Å	1.537	1.544	I:1.537 II:1.570	I:1.573 II:1.548 III:1.542	I:1.548 II:1.539 III:1.562	1.420

Then we calculate the work functions of all the structures, as shown in Fig.2. Work function is usually defined as the minimum energy needed to take an electron away from the Fermi level to the vacuum level [10]. Work function can be measured accurately by the Kelvin probe force microscopy [11]. The average planar electrostatic potentials (APEPs, Fermi level is set to be reference) of all the systems are shown in Fig.2. The calculated work functions of all systems including pristine graphene are listed in Tab. I. All the structures are symmetrical in the orientation of z axis and the surface work functions are equal for both sides of the system, as shown in Fig.2. We can get the information that the work function varies with the different configurations. For example, the work function of boat1 is only about 4.417eV, whereas the work function of boat3 is up to 4.543eV. This can be used to distinguish those two structures by using scan tunneling microscope (STM).

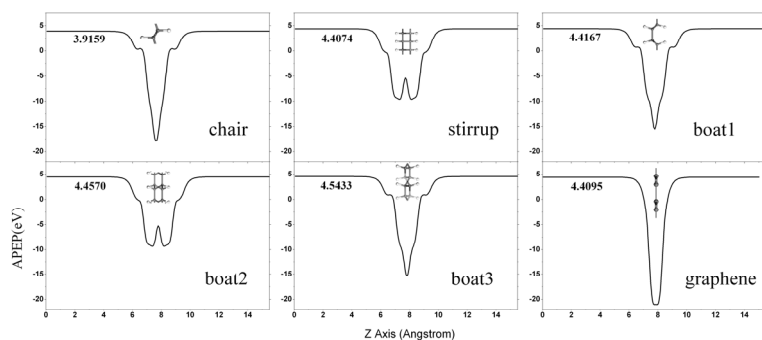


Figure.2 The work functions of the graphene and the hydrogenated graphene.

Conclusion

In summary, we have studied the structures and work functions of the hydrogenated graphene by first-principles calculations. The difference of the work function and the thickness of the structure, which induced by the different hydrogenated configurations, may provide a criterion for identifying these configurations.

Acknowledgment

This work is supported by the National Natural Science Foundation of China (Grant Nos. 10874143), the Program for New Century Excellent Talents in University (Grant No. NCET-10-0169), and the Scientific Research Fund of Hunan Provincial Education Department (Grant Nos. 10K065).

- (1) K. S. Novoselov, A. K. Geim, S. V. Morozov, D. Jiang, Y. Zhang, S. V. Dubonos, I. V. Grigorieva, A. A. Firsov, *Science* 2004 306, 666.
- (2) B. Obradovic, R. Kotlyar, F. Heinz, P. Matagne, T. Rakshit, M. D. Giles, M. A. Stettler, *Appl. Phys. Lett.* 2006 88, 142102.
- (3) D. Gunlycke, D. A. Areshkin, Junwen Li, J. W. Mintmire, C. T. White, *Nano Lett.* 2007 7, 3608.
- (4) G. C. Liang, N. Neophytou, D. E. Nikonov, M. S. Lundstrom, *IEEE Trans. Electron Devices* 2007 54, 677.
- (5) J. C. Meyer, A. K. Geim, M. I. Katsnelson, K. S. Novoselov, T. J. Booth, S. Roth, *Nature* 2007 446, 60.
- (6) J. O. Sofo, A. S. Chhauhari, G. D. Barber, *Phys. Rev. B* 2007 75, 153401.
- (7) O. Leenaerts, H. Peelaers, A. D. Hernández-Nieves, B. Partoens, F. M. Peeters, *Phys. Rev. B* 2010 82, 195436.
- (8) Xiao-Dong Wen, Louis Hand, Vanessa Labet, Tao Yang, Roald Hoffmann, N. W. Ashcroft, Artem R. Oganov, Andriy O. Lyakhov, *PANS* 2011 108, 6833.
- (9) G. Kresse, J. Furthmüller, *Phys. Rev. B* 1996 54, 11169.
- (10) N. D. Lang, *Phys. Rev. B* 1971 4, 4234.
- (11) M. Nonnenmacher, M. P. OBoyle, and H. K. Wickramasinghe, *Appl. Phys. Lett.* 1991 58, 2921.